Current Trends in Biotechnology and Pharmacy
Vol. 20 (Supplementary Issue 2A), June 2026, ISSN 0973-8916 (Print)., 2230-7303 (Online)
10.5530/ctbp.2026.2s.1

In silico evaluation of flavanones as anti-psoriatic agents targeting inflammatory pathways: Molecular docking studies and ADMET profiling

Narendra Pentu[1,2], and Manikanta Murahari[1]*

[1]Department of Pharmaceutical Chemistry,KL College of Pharmacy, Koneru Lakshmaiah Educational Foundation, Vaddeswaram, Guntur-522502, Andhra Pradesh, India

[2]Department of Pharmaceutics, CMR College of Pharmacy, Kandlakoya(V), Medchal, Hyderabad-501401, Telanganam India

*Corresponding author: manikantam@kluniversity.in

Abstract

Background: Flavanones, a subclass of polyphenolic secondary metabolites, exhibit significant anti-inflammatory, antioxidant, and antiproliferative properties relevant to psoriasis therapy. Structure-based drug design through molecular docking enables prediction of ligand–protein interactions by estimating binding affinities and characterizing key non-covalent interactions, thus facilitating the identification of flavanone scaffolds with prospective anti-psoriatic potential. Method: AutoDock Vina was used to dock flavanone ligands against psoriasis-related protein targets, predicting binding affinities and interaction profiles relative to standard inhibitors. In silico pharmacokinetic and ADMET properties were assessed using pkCSM and SwissADME to evaluate drug-likeness and optimize lead selection. Results: Narirutin and Hesperidin exhibited strong binding affinity towards the psoriasis targets, while Hesperidin, Neoeriocitrin, Narirutin, Neohesperidin, and Poncirin showed Lipinski's violation and lower ADMET profiles. Hierarchical cluster dendrogram and similarity network give a detailed data set analysis. Conclusion: High-throughput screening enables rapid, cost-effective drug discovery. Flavanones demonstrated superior in silico anti-psoriatic activity compared to standard drugs, though low solubility limits bioavailability. Nanoformulations could enhance target-site delivery, and further clinical studies are needed to develop these plant-derived compounds into effective therapeutics.

Keywords: Molecular docking studies, ADMET profiling, Psoriasis, Flavanones, Redocking.

Introduction

Psoriasis is a persistent inflammatory skin disease marked by abnormal keratinocyte proliferation, resulting in erythematous plaques and scaly lesions on the epidermis. The condition is primarily mediated by proinflammatory cytokines and the infiltration of immune cells. The underlying cause of the disease is still unclear; however, genetic, environmental, and lifestyle factors play an important role in its initiation. Although psoriasis is not life-threatening, it is frequently associated with comorbidities such as psoriatic arthritis, cardiovascular disease, irritable bowel syndrome, and other immune-mediated inflammatory disorders (1). Epidemiological patterns and prevalence rates of psoriasis depend on the severity and clinical presentation of the disease (2). Topical, physical, systemic, and biological treatments have shown good effects to improve the disease condition, but have not completely cured it. Out of the available treatments, biologics are the current highly prescribed medications with more or less side effects. Lifelong medication may affect the socio-economic and psychological condition of the patients (3).

Several researchers are elucidating molecular disease pathways to better understand and modify the condition. Psoriasis pathogenesis is strongly influenced

Vol. 20 (Supplementary Issue 2A), June 2026, ISSN 0973-8916 (Print)., 2230-7303 (Online)
10.5530/ctbp.2026.2s.1

by the TNF-α/IL-23/IL-17 axis, which induces inflammation and stimulates keratinocyte hyperproliferation (4). Under normal conditions, keratinocytes are produced daily to replace dead cells in the skin. In psoriasis, however, their hyperproliferation results in scaly skin, itching, and occasional bleeding. The Psoriasis Area and Severity Index (PASI) is a standardized clinical assessment tool used to determine the severity of psoriasis by evaluating scaling, erythema, and lesion thickness. The scoring ranges from 0 to 4, where 0 denotes no disease activity and 4 indicates severe involvement. The treatment timeline of psoriasis highlights the progressive evolution of therapeutic strategies: 1920s (coal tar, salicylic acid), 1950s (fumaric acid, methotrexate), 1970s (cyclosporine, PUVA), 1980s (phototherapy, retinoic acid), 2000s (T-cell–targeted biologics), and 2010s (novel small-molecule inhibitors)(5)(6).

Flavanones are a subclass of flavonoids and represent secondary metabolites derived from plants (7,8)Flavonoids primarily function in plants to enhance immunity, protect against environmental stress, and support overall growth by facilitating nutrient availability. Flavanones, a subclass of flavonoids, are mostly present in citrus fruits (family Rutaceae) such as lemons, oranges, limes, and grapefruits. They are also commonly referred to as bioflavonoids or citrus polyphenols (9)(10). Flavonoid compounds reduce skin inflammation and enhance dermal penetration (11). Bioactive compounds in the diet can help lower the risk of disease, such as flavanones (12).

Flavanones are a subclass of flavonoids characterized by a 15-carbon skeleton consisting of two aromatic rings, A (Typically hydroxylated at positions 5 and 7) and B (Substitutions at C3′, C4′, or C5′ (often hydroxyl or methoxy groups) connected by a three-carbon heterocyclic C-ring with a ketone group at position 4. Unlike flavones, flavanones have a saturated C2–C3 bond in the heterocyclic ring (13).

Pharmacokinetics and Absorption of Flavanones

Flavanone absorption plays a key role in their pharmacokinetic profile. Mainly, passive diffusion governs the absorption process due to their relatively low MW, high lipophilicity (logP: 2.3–2.7), and weakly acidic nature (14),(15). Glycosylation of flavanones increases hydrophilicity, thereby reducing absorption via passive diffusion (16). Flavanones are classified into three subcategories based on glucose conjugation: aglycones, monoglucosides, and diglucosides. Aglycone flavanones can conjugate with β-glucuronidase and enter paracellular transport through passive diffusion. Flavanone-7-O-glucosides are converted to aglycones via two pathways: (i) hydrolysis by lactase-phlorizin hydrolase (LPH) at the intestinal brush border, and (ii) transport via glucose transporters, followed by hydrolysis with cytosolic β-glucosidase, forming flavanone glucuronides or sulfates, which then enter paracellular transport via multidrug resistance proteins (MDR1–3). The free 7-OH group in flavanone aglycones enhances binding interactions with human serum albumin (HSA). In contrast, flavanones with a 7-O-glucose moiety show reduced binding due to increased hydrophilicity, which limits interaction with the hydrophobic cavity of HSA. Flavanones tend to accumulate in the liver following absorption (17,18).

The current study sought to assess the anti-psoriatic potential of flavanones by computational methods. AutoDock Vina was used for molecular docking to investigate the affinity of flavanone ligands for target protein molecules. Furthermore, the pharmacokinetic and toxicity profiles of the drugs were evaluated using the pkCSM and SwissADME tools.

Materials and Methods

Database servers, including PubMed, PubChem, Protein Data Bank (PDB), Google Scholar, and Medline, were utilized to access relevant data. PubMed and Google Scholar were employed to identify potential literature supporting the present work. Chemical

Vol. 20 (Supplementary Issue 2A), June 2026, ISSN 0973-8916 (Print)., 2230-7303 (Online)
10.5530/ctbp.2026.2s.1

structures of the selected compounds in SDF format were collected from PubChem for molecular docking experiments, while three-dimensional protein structures were obtained from the PDB repository. Molecular docking was performed using AutoDock Tools 1.5.7 for receptor preparation, followed by docking with AutoDock Vina (19). Pharmacokinetic and toxicity predictions were assessed using the pkCSM web server (https://biosig.lab.uq.edu.au/pkcsm/) and SwissADME (http://www.swissadme.ch/). The docking poses and molecular interactions were visualized with BIOVIA Discovery Studio Visualizer. All computational studies were carried out on a 64-bit Windows 11 system equipped with 16 GB RAM and a 13th Generation Intel® Core i5-1335U (1.30 GHz, x64 architecture) (20).

Docking protocol

Protein preparation

Psoriasis-associated proteins' crystal structures were obtained from the Protein Data Bank (PDB). The co-crystallized ligand and water molecules were removed to prepare the receptor, allowing the experimental ligand to be docked into the corresponding binding site. The space vacated by the native ligand was defined using a spherical grid to calculate the docking coordinates. These coordinates were then employed to dock the experimental ligand into the prepared protein structure. Docking involved calculating docking scores and identifying interactions, such as hydrogen bonds and other contacts, between the ligand and the protein's amino acid residues.

Ligand preparation

Ligand structures were extracted from the PubChem database in SDF format and translated to PDB using OpenBabel. The generated PDB files were then converted into PDBQT format using AutoDock Tools 1.5.7 to prepare for molecular docking investigations (Fig. 1 and Table 1) (21).

Docking studies

Molecular docking is a computer technique for predicting the binding affinity and orientation of ligands within the active site of a target protein. The docking simulations in this work were performed using AutoDock Vina. The protein structure remained rigid, while the ligands were considered as flexible, permitting rotation around their rotatable bonds (Table 2). The binding interactions were assessed based on docking scores, which indicate the strength and stability of the non-covalent interactions between the ligand and the protein (22).

LigandFit was utilized to connect ligands to the target proteins' active regions. Protein preparation included removing water molecules, constructing a docking grid, and removing the co-crystallized ligand. The resulting protein structure was saved in the PDBQT format. Docking was performed by introducing the ligand into the native ligand pocket, allowing interactions with the amino acid residues present at the binding site with structure-based drug design. A two-dimensional interaction diagram was then developed to depict non-covalent bonds, the matching amino acid residues, and bond lengths (23).

Docking validation

Molecular docking validation was carried out by re-docking the co-crystallized ligand in the protein. A small molecule from the protein-ligand complex was extracted to do the redocking procedure (24,25).

Drug-like properties

According to Lipinski's Rule of Five, an orally active drug candidate should comply with specific physicochemical properties to ensure better absorption and bioavailability in systemic circulation. (Refer to Table 3) Compounds violating more than one of these rules are likely to exhibit poor oral absorption or permeation (26).

According to the Veber rule, drug molecules should have rotatable bonds <10, TPSA is <140 to exhibit the highest oral bioavailability (27). Ghose rule predicts the drug-like properties based on the following conditions: molecular weight (160 to 480 Da), partition coefficient (-0.4 to + 5.6), Molar

Vol. 20 (Supplementary Issue 2A), June 2026, ISSN 0973-8916 (Print)., 2230-7303 (Online)
10.5530/ctbp.2026.2s.1

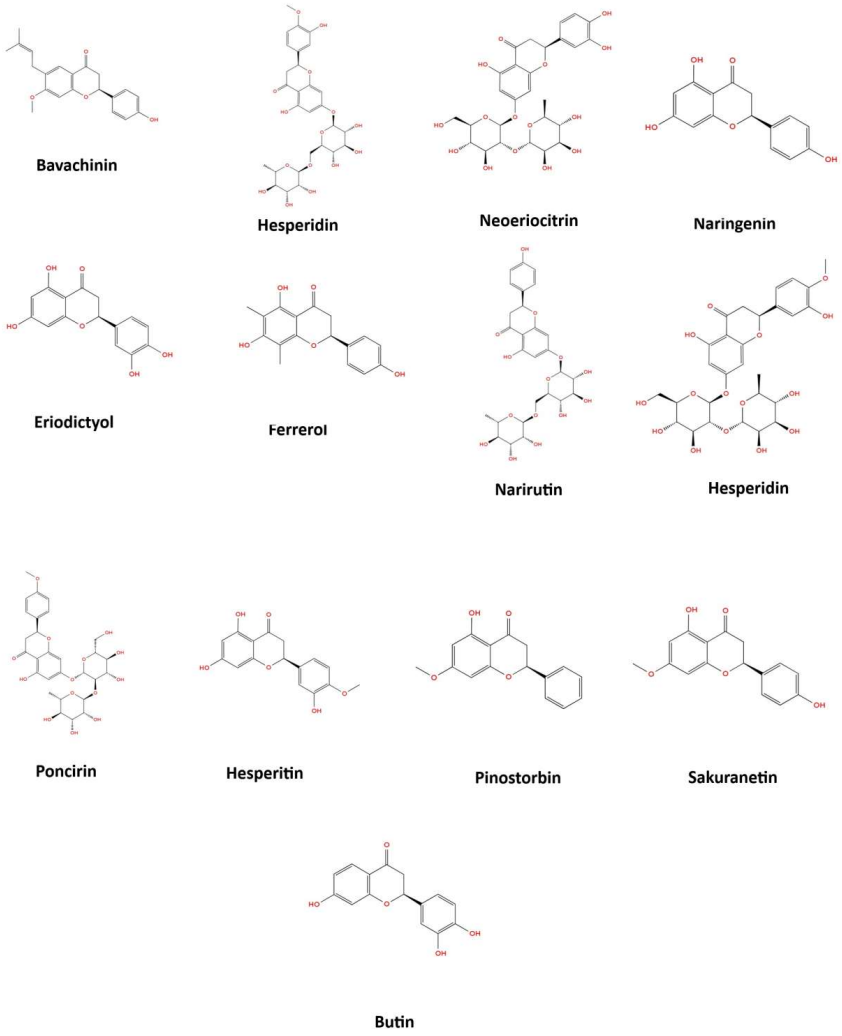

Fig. 1: Structures of Flavanone

refractivity (40 to 130), and total number of atoms between 20 and 70 (28).

Toxicity studies

Drug toxicity profiles were assessed using pkCSM software to predict pharmacokinetic and toxicity features. The analysis includes investigations on absorption, distribution, metabolism, excretion, and toxicity (ADMET) (29).

Results & Discussion

Pharmacokinetic and Toxicity study with drug-like properties

According to the docking protocol, the docking studies were carried out and further extended to visualize the structural features and bonding interactions between the protein and amino acid residues. The drug-likeness properties are presented in Table 4, providing the molecular descriptors that indicate the

Vol. 20 (Supplementary Issue 2A), June 2026, ISSN 0973-8916 (Print)., 2230-7303 (Online)
10.5530/ctbp.2026.2s.1

potential for absorption through the oral route of administration.

GRID generation

After visualizing the protein structure in Discovery Studio, the binding site was identified based on the position of the native ligand within the protein. The coordinates and binding site attributes of the native ligand were recorded, after which the ligand was removed to obtain the apo form of the protein. The prepared protein was then used for molecular docking studies to analyze and predict the interactions between the receptor and the selected ligands (Table 5).

Molecular docking studies

The protein molecules acquired from Discovery Studio after ligand removal were loaded into Autodock Vina for molecular docking analysis. Ligand structures were created individually and then converted to PDBQT format using Open Babel. The protein's active site was defined by entering

Table 1: Flavanones with their PubChem ID

Ligand	PubChem ID
Bavachinin	10337211
Butin	92775
Eriodictyol	440735
Farrerol	442396
Hesperidin	10621
Hesperitin	72281
Naringenin	439246
Narirutin	442431
Neoeriocitrin	114627
Neohesperidin	442439
Pinostrobin	73201
Poncirin	442456
Sakuranetin	73571

Table 3: Rule of five to predict the drug-like properties

Molecular Property	Limit Value
MW	< 500 Da
Lipophilicity	≤ 5 (typically 3-5)
HBA	≤ 10
HBD	≤ 5

Table 2: Crystallographic structures of proteins and their specification

Protein	PDB ID	Organism	Resolution	R value free	Method
IL-23	3QWR	Homosepians	3.25 Å	0.264	X-Ray Diffraction
IL-17A	5HI4	Homosepians	1.80 Å	0.224	X-Ray Diffraction
BTK	4OTF	Homosepians	1.95 Å	0.203	X-Ray Diffraction
PDE-4	5K1I	Homosepians	2.61 Å	0.258	X-Ray Diffraction
TNF-α	2AZ5	Homosepians	2.10 Å	0.278	X-Ray Diffraction
AA_2R	2YDO	Homosepians	3.00 Å	0.269	X-Ray Diffraction
JAK-3	5TTS	Homosepians	2.34 Å	0.263	X-Ray Diffraction
PAD	4X8G	Homosepians	3.29 Å	0.230	X-Ray Diffraction
P38MAP kinase	3QUE	Homosepians	2.70 Å	0.311	X-Ray Diffraction

Vol. 20 (Supplementary Issue 2A), June 2026, ISSN 0973-8916 (Print)., 2230-7303 (Online)
10.5530/ctbp.2026.2s.1

Table 4: Molecular descriptors value of Flavanones

S. No.	Compound	HBA	HBD	Mol. Wt	X logP	R.Bonds	TPSA	Molar Ref.	No. of Atoms
1	Bavachinin	4	1	338.403	4.616	4	147.260	97.74	25
2	Hesperidin	15	8	610.565	-1.1566	7	244.507	141.41	43
3	Neoeriocitrin	15	9	596.538	-1.4596	6	237.822	136.94	42
4	Naringenin	5	3	272.256	2.5099	1	114.235	71.57	20
5	Eriodictyol	6	4	288.255	2.215	1	119.029	73.59	21
6	Farrerol	5	3	300.31	3.126	1	126.965	81.50	22
7	Narirutin	14	8	580.539	-1.1652	6	233.028	134.91	41
8	Neohesperidin	15	8	610.565	-1.1566	7	244.507	141.41	43
9	Poncirin	14	7	594.566	-0.8622	7	239.713	139.38	42
10	Hesperitin	6	3	302.282	2.5185	2	125.714	78.06	22
11	Pinostrobin	4	1	270.284	3.1073	2	116.125	74.02	20
12	Sakuranetin	5	2	286.283	2.8129	2	120.920	76.04	21
13	Butin	5	3	272.256	2.5099	1	114.235	71.57	20

the required grid box coordinates, and the processed protein structure was saved in PDBQT format. Before docking, polar hydrogens and partial charges were introduced into the protein structure. Docking simulations were then performed, and the binding affinities of the protein–ligand complexes were evaluated based on their docking scores (Fig. 2).

Discussion

Drug-like properties

Drug-like properties are disclosed, including the data relevant to drug absorption through the oral route of administration. As per the rule of five, molecular descriptors like weight, logP, HBA, and HBD should be within the range of Lipinski's rule of five to exhibit the desired property (30) Hesperidin, Neoeriocitrin,

Vol. 20 (Supplementary Issue 2A), June 2026, ISSN 0973-8916 (Print)., 2230-7303 (Online)
10.5530/ctbp.2026.2s.1

Table 5: Predicted ADMET values of Flavanone compounds

Properties	C'1	C'2	C'3	C'4	C'5	C'6	C'7	C'8	C'9	C'10	C'11	C'12	C'13
Solubility	-4.916	-3.014	-2.9	-3.2224	-3.2353	-3.3327	-3.0038	-2.8776	-2.97	-3.0047	-3.4445	-3.14	-3.4333
CaCo2 Permeability	1.253	0.505	-0.855	1.029	-0.094	1.22	0.521	0.57	0.612	0.294	1.296	1.364	1.172
Intest. absorption	93.672	31.481	16.143	91.31	74.687	91.927	36.625	20.652	30.305	70.277	93.762	92.601	93.171
Skin Permeation	-2.79	-2.735	-2.735	-2.742	-2.735	-2.737	-2.735	-2.735	-2.735	-2.737	-2.757	-2.76	-2.738
PgP-substrate	1	1	1	1	1	1	1	1	1	1	0	1	1
PgP- I Inhibitor	1	0	0	0	0	0	0	0	1	0	0	0	0
PgP-II Inhibitor	0	0	0	0	0	0	0	0	0	0	0	0	0
VDss	0.398	0.996	0.827	-0.015	0.377	0.791	1.295	0.348	-0.058	0.746	-0.248	-0.054	0.511
Unbound fraction	0	0.101	0.178	0.064	0.106	0.106	0.121	0.148	0.146	0.118	0.032	0.034	0.124
BBB Permeation	-0.36	-1.715	-1.836	-0.578	-0.827	-0.777	-1.594	-1.72	-1.584	-0.719	0.085	-0.216	-0.753
CNS Permeation	-1.878	-4.807	-4.925	-2.215	-3.142	-2.036	-4.708	-4.872	-4.732	-2.976	-2.072	-2.251	-2.251
CYP2D6 substrate	0	0	0	0	0	0	0	0	0	0	0	0	0

Vol. 20 (Supplementary Issue 2A), June 2026, ISSN 0973-8916 (Print)., 2230-7303 (Online)
10.5530/ctbp.2026.2s.1

CYP3A4 substrate	1	0	0	0	0	0	0	0	0	0	1	0	0
CYP1A2 inhibitor		0	0	1	0	1	0	0	0	0	1	1	1
CYP2C19 inhibitor	1	0	0	0	0	1	0	0	0	0	1	1	0
CYP2C9 inhibitor	1	0	0		0	1	0	0	0	0	0	0	0
CYP2D6 inhibitor	0	0	0	0	0	0	0	0	0	0	0	0	0
CYP3A4 inhibitor	1	0	0	0	0	0	0	0	0	0	0	0	0
Total clearance	0.073	0.211	0.125	0.06	-0.013	0.07	0.307	0.222	0.419	0.044	0.236	0.174	-0.008
Renal OCT2 substrate	0	0	0	0	0	0	0	0	0	0	0	0	0
AMES tox	0	0	0	0	0	0	0	0	0	0	1	0	0
Max. tolerable dose	0.03	0.525	0.475	-0.176	0.014	-0.207	0.467	0.389	0.259	0.25	0.26	-0.031	-0.171
hERG I inhibitor	0	0	0	0	0	0	0	0	0	0	0	0	0
hERG II inhibitor	1	1	1	0	0	0	1	1	1	0	0	0	0

Vol. 20 (Supplementary Issue 2A), June 2026, ISSN 0973-8916 (Print)., 2230-7303 (Online)
10.5530/ctbp.2026.2s.1

Liver tox	0	0	0	0	0	0	0	0	0	0	0	0	0
SS	0	0	0	0	0	0	0	0	0	0	0	0	0
LD_{50}	2.217	2.506	2.487	1.791	2.03	2.327	2.519	2.479	2.545	2.042	2.152	2.172	2.33
LOAEL	1.257	3.167	4.385	1.944	2.475	1.703	3.203	4.149	4.096	2.605	1.893	2.07	2.022
# C1 to C13 represents the- Bavachinin, Hesperidin, Neoeriocitrin, Naringenin, Eriodictyol, Ferrerol, Narirutin, Neohesperidin, Poncirin, Hesperitin, Pinostrobin, Sakuranetin and Butin. * Here '0' indicates "No" and '1' indicates "Yes". SS- Skin sensitization													

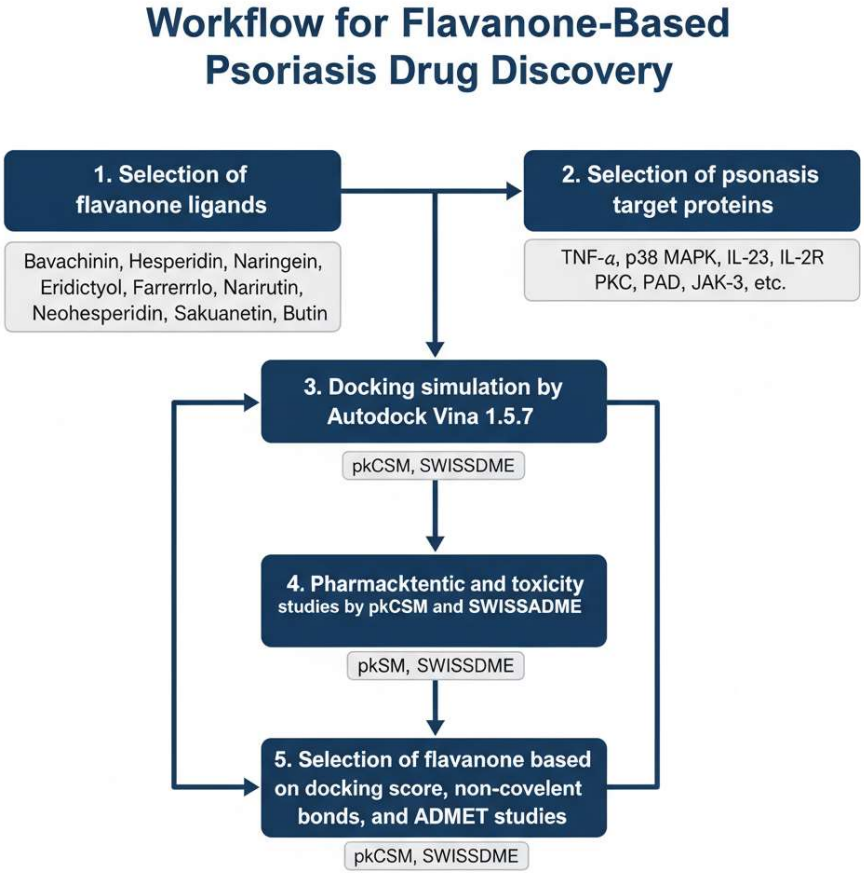

Fig. 2: Graphical representation of the molecular docking studies workflow

In silico evaluation of flavanones

Vol. 20 (Supplementary Issue 2A), June 2026, ISSN 0973-8916 (Print)., 2230-7303 (Online)
10.5530/ctbp.2026.2s.1

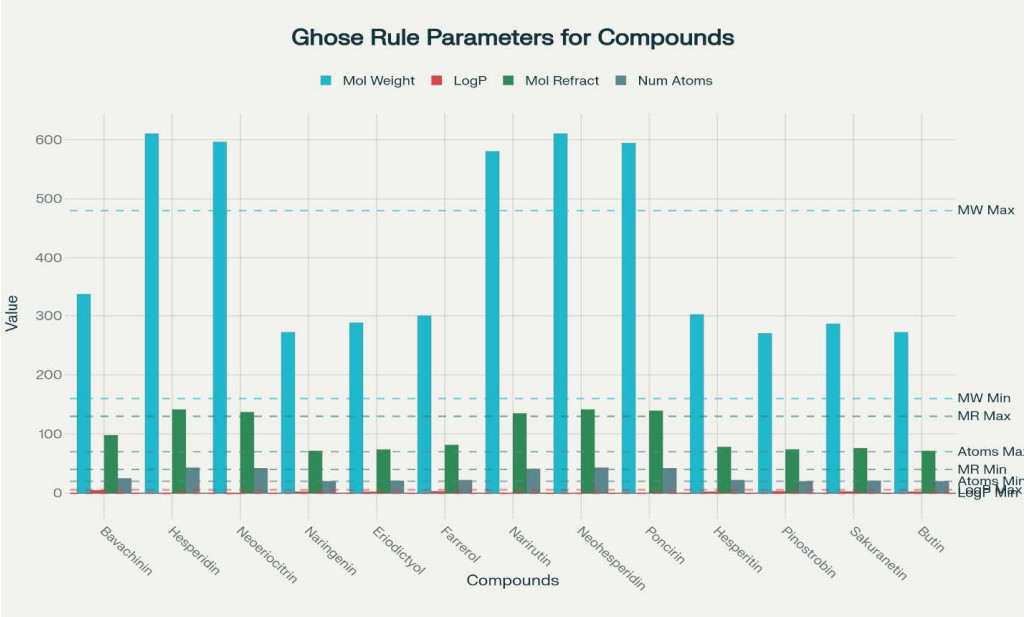

(a) Ghose rule

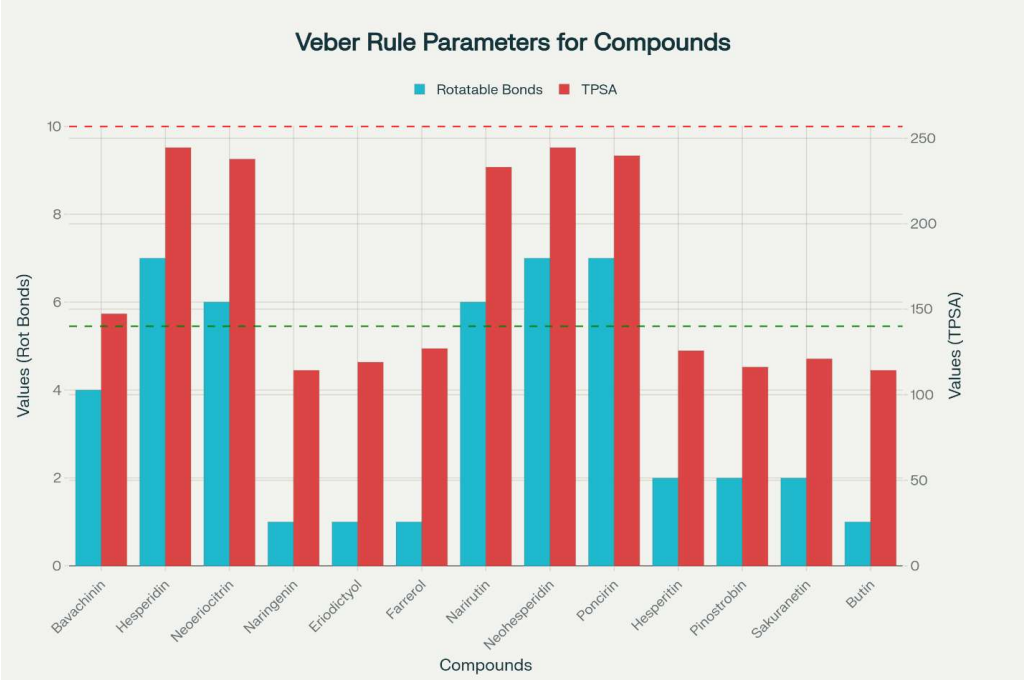

(b) Veber rule of drug likeness properties

Vol. 20 (Supplementary Issue 2A), June 2026, ISSN 0973-8916 (Print)., 2230-7303 (Online)
10.5530/ctbp.2026.2s.1

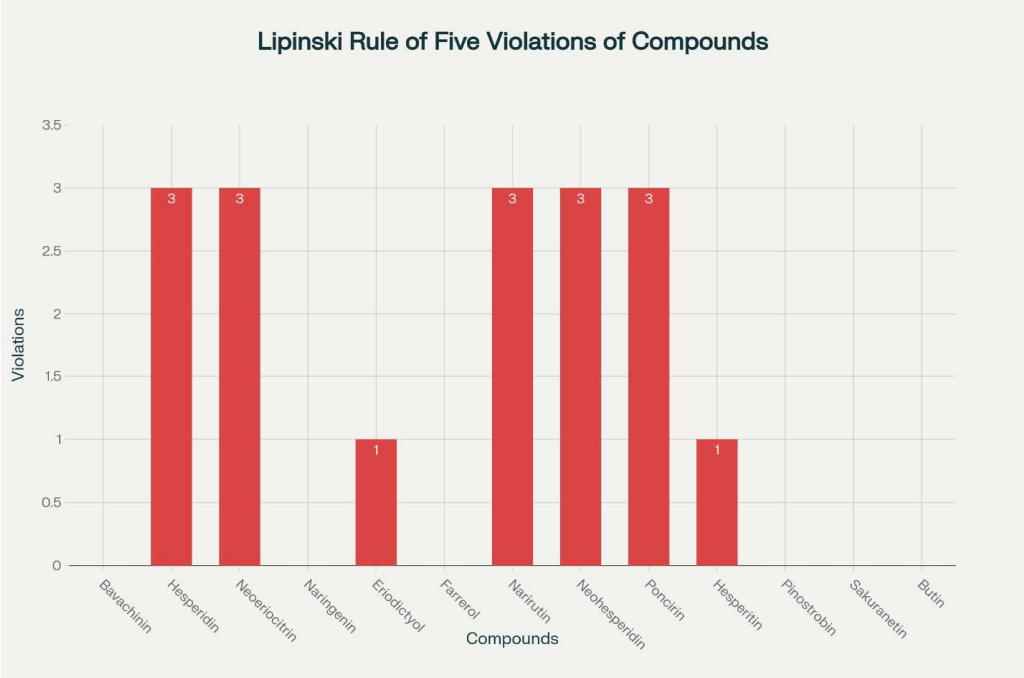

(c) Lipinski rule of five

Fig. 3: Drug-like properties represented in graphical format

Narirutin, Neohesperidin, and Poncirin exhibited the highest number of violations (three in total). According to Lipinski's Rule of Five, compounds with more than one violation are unlikely to be delivered effectively through the oral route of administration. As per the Ghose and Veber rules, the above-mentioned compounds were found to violate the established criteria (Fig. 3) (31).

Kinetics and toxicity studies

Toxicity profiles of the flavanones are studied to estimate the safety features of the drug molecules. Total pharmacokinetic and toxicity profiles are described in Table 6, colored portions are indicated as violations against the regular limitations proposed by various studies. PSA< 140, logP<5 are the specifications to improve the solubility and permeation. Compounds C1, C2, C3, C7, C8, and C9 exhibited PSA values exceeding the acceptable limit, indicating poor lipid solubility and limited ability to cross the plasma membrane via passive diffusion. Absorption characteristics such as Papp permeability values greater than 0.90 indicate better permeation, intestinal absorption values above 30% suggest good absorption, while skin permeability values lower than –2.5 are considered to indicate low skin permeation. Compounds C3a and C8 have the lowest intestinal absorption values. All the molecules have an affinity to bind with the Pgp protein. Drug molecules with VDss values below –0.15 indicate a better volume of distribution. A BBB value greater than 0.3 suggests that the compound can easily cross the blood–brain barrier, while values below 3 indicate efficient penetration into the CNS. The studied chemicals had minimal ability to penetrate the BBB, with naringenin in particular exhibiting little capacity to

Vol. 20 (Supplementary Issue 2A), June 2026, ISSN 0973-8916 (Print)., 2230-7303 (Online)
10.5530/ctbp.2026.2s.1

Table 6: Protein code with GRID coordinates	
Protein	GRID
3QWR	24.346980 - 28.225320 - 51.874320
5HI4	80.731080 - 43.501432 - 45.735545
4OTF	-38.572442 27.147767 - 10.124349
5K1I	12.576071 3.744179 67.719607
2AZ5	-19.409600 74.650750 33.849550
2YDO	-29.604000 8.482211 -22.855421
5TTS	-0.164050 16.815400 -4.872050
4X8G	27.438969 44.051375 26.640750
3QUE	-24.576650 - 12.535900 8.792250

permeate the CNS. All of the medication compounds had low clearance rates from the human body, which might be explained by their water solubility and molecular weight. There was no detectable AMES toxicity, indicating that gene mutation is unlikely. However, naringin and hesperidin molecules were shown to inhibit hERG II. Modifying these compounds' structural moieties can improve their solubility and drug permeability capabilities (32).

The hERG II inhibitory action is coupled with cardiotoxicity, which can be reduced by structural modifications to the compounds. Simultaneous injection of hERG channel blockers may also aid in decreasing interactions with this channel. The flavanone compounds showed no evidence of hepatotoxicity or skin sensitivity.

Redocking

Redocking was performed with the native ligand, and the RMSD values were recorded as < 2 with the successful docking accuracy when compared with the experimental results (33).

Hierarchical Cluster Analysis Using Drug-Likeness and ADMET Properties

The selected compounds were classified using hierarchical cluster analysis (HCA) based on their pharmacokinetic and drug-likeness properties. The dendrogram Figure 4 shows two significant clusters with differing grouping patterns based on similarities in ADMET profiling parameters.

The first cluster (green branch) consists of chemicals C3, C8, C7, C2, and C9, which have very similar physicochemical and pharmacokinetic properties. These compounds have good oral bioavailability and balanced lipophilicity, indicating good membrane permeability and metabolic stability. The cluster's modest linkage lengths imply minimal diversity in drug-likeness features.

The second cluster (red branch) contains chemicals C4, C6, C1, C11, C12, C13, C5, and C10, which exhibit unique ADMET behavior from the first group. The internal distances within this cluster remain low, indicating that these substances are highly comparable in terms of solubility, clearance rate, and toxicity risk. This cluster may comprise drugs with enhanced safety profiles and a lower hERG inhibition potential (34).

Overall, the clustering pattern distinguishes the drugs based on their ADMET and drug-likeness profiles, revealing two pharmacokinetically separate groupings. This classification helps identify lead compounds with high bioavailability, low toxicity, and favorable drug-like behavior for further optimization in the drug development process.

Flavanone Compounds Represented in Network Graphs

With clusters resulting from dendrograms transferred into a circular node architecture, the network graph illustrates the

Vol. 20 (Supplementary Issue 2A), June 2026, ISSN 0973-8916 (Print)., 2230-7303 (Online)
10.5530/ctbp.2026.2s.1

linkages and resemblance patterns among flavanone chemicals based on hierarchical clustering analysis.

Flavanone compounds (C1–C13) are represented by each node, while cluster-based associations deduced from the original dendrogram are shown by edges (Fig. 5). Regardless of cluster size, the circular arrangement guarantees consistent visual emphasis on all compounds, making it easier to comprehend connectedness. Similar to similarity scores, edge labels indicate how near compound pairs are to one another based on their hierarchical clustering distances. It makes it possible to identify hub molecules with numerous connections, indicating key functions in the network and possible prioritization for more pharmacological or ADMET research. These network-based insights can direct optimization tactics, structural analysis, and chemical selection.

SAR analysis and molecular docking

Significant discrepancies in binding affinities were found when flavonoid molecules were molecularly docked to a variety of target receptors. This suggests that the receptor interactions of flavonoids are influenced by small structural differences (Fig. 6).

The drugs that showed the strongest docking affinity for the PDE-4 receptor among the tested were narirutin (-11.0 kcal/mol) and hesperidin (-11.2 kcal/mol), indicating strong inhibitory potential. The compounds' dual target potential was demonstrated by their significant interactions with the BTK receptor (-10.3 kcal/mol). These compounds' high binding affinity may be attributed to the presence of many hydroxyl and glycosidic moieties, which seem to improve hydrogen bonding and electrostatic interactions within the receptor binding pocket.

However, out of all the ligands, IL-23 had the lowest docking scores, indicating little interaction and a poor preference for these flavonoid scaffolds for binding. The importance of the sugar-replaced flavanone backbone in stabilizing receptor binding is further supported by compounds like Neohesperidin, Neoeriocitrin, and Poncirin, which likewise showed good docking scores (about -9.8 to -10.1 kcal/mol) with PDE-4 and BTK. Simple flavonoids, such as Butin, Sakuranetin, and Pinostrobin, on the other hand, showed comparatively weaker interactions across targets. This is probably because they lack glycosidic substitutions, which restrict the ability to form hydrogen bonds. From a structure-activity standpoint,

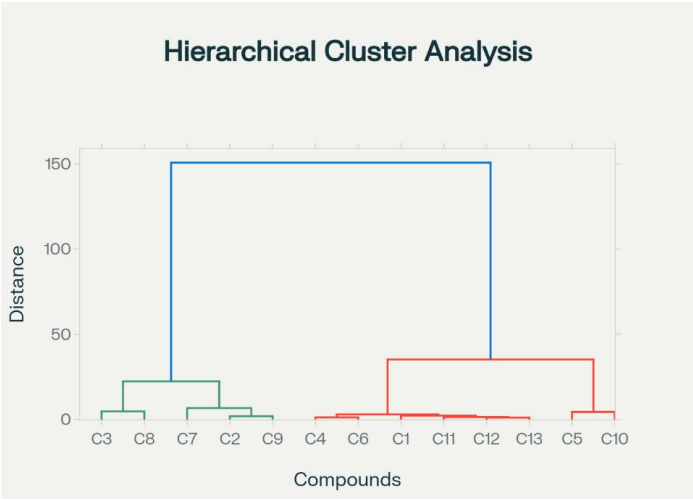

Fig. 4: Hierarchical clustering of flavanones based on drug-likeness and ADMET properties

In silico evaluation of flavanones

Vol. 20 (Supplementary Issue 2A), June 2026, ISSN 0973-8916 (Print)., 2230-7303 (Online)
10.5530/ctbp.2026.2s.1

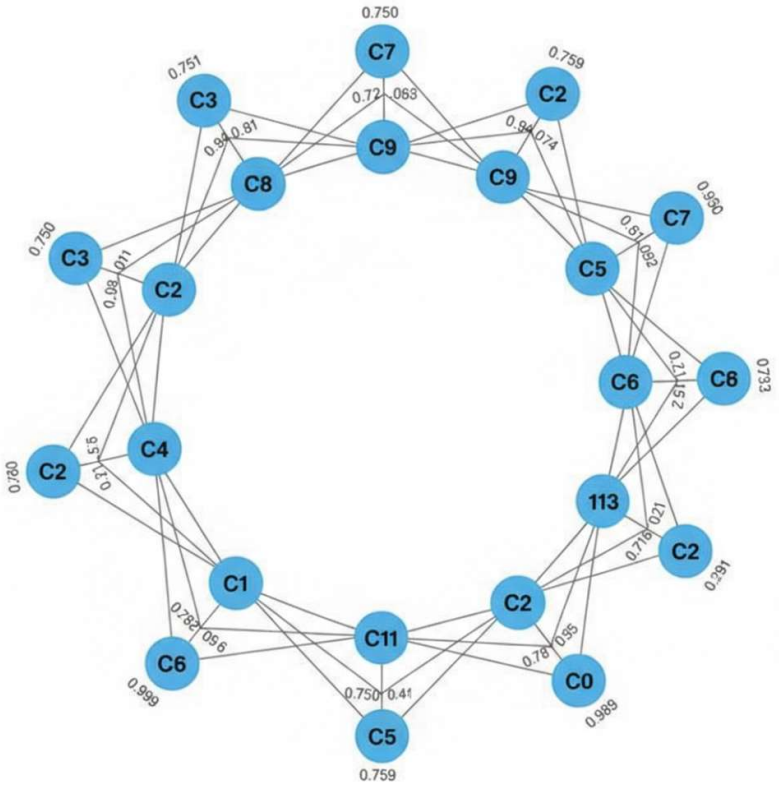

Fig. 5: ADMET similarity network for the C1 to C13 compounds data set

the findings indicate that enhanced hydroxylation and glycosylation improve binding affinity, particularly toward PDE-4 and BTK receptors, which are important mediators in inflammatory signalling pathways. These findings highlight the pharmacophoric importance of polar substituents in enhancing molecular interactions and target specificity. Overall, Hesperidin and Narirutin emerge as leading flavanone candidates with broad-spectrum receptor affinity, showing their potential as anti-inflammatory medicines via multi-target regulation.

Natural flavanone chemicals, such as naringenin, hesperidin, and narirutin, have been shown to bind significantly to protein targets relevant to psoriasis, such as IL-17A, IL-23, TNF-α, and kinases. Docking scores vary from -7.0 to -11.2 kcal/mol, showing significant binding affinity and competitive suppression of inflammatory pathways. Notably, when flavonoids are coupled with biologic medicines, synergistic effects have been seen, which increase cytokine suppression while also enhancing overall treatment outcomes. Natural substances, particularly flavanones found in foods or herbal supplements, present a viable alternative for psoriasis treatment. Flavanones and their analogs, notably naringenin and hesperetin, have anti-inflammatory and antioxidant activities, targeting important signaling pathways such as STAT3, JAK, and TNF-α. They help limit keratinocyte proliferation and cytokine overproduction, resulting in symptomatic alleviation, fewer problems, and better skin barrier healing.

Vol. 20 (Supplementary Issue 2A), June 2026, ISSN 0973-8916 (Print)., 2230-7303 (Online)
10.5530/ctbp.2026.2s.1

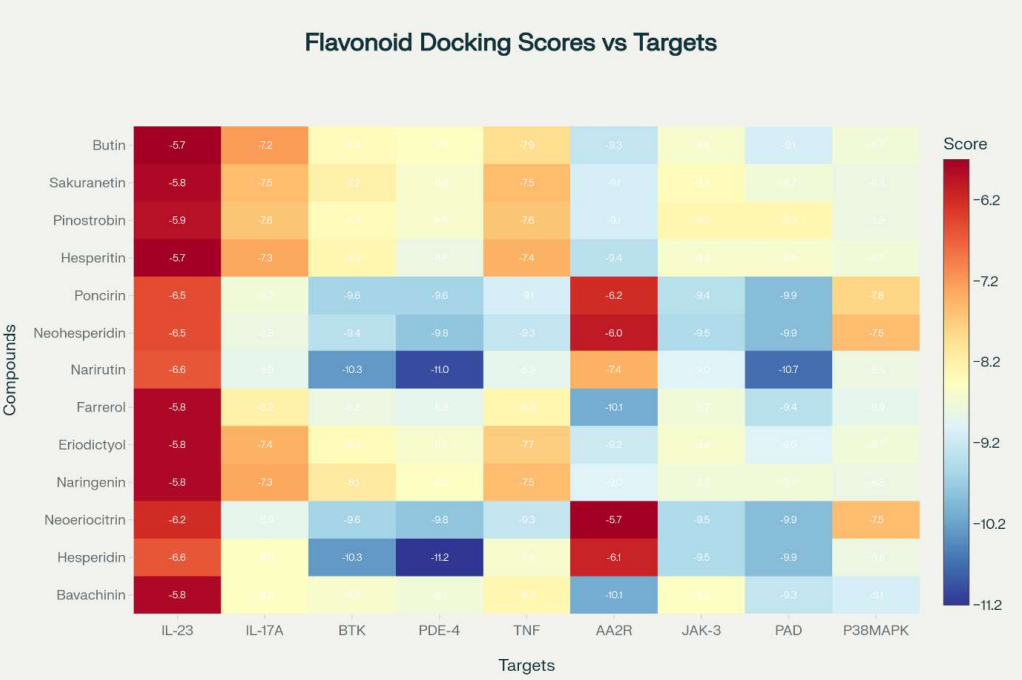

Fig. 6: Docking scores of the receptors with their respective ligands are represented in the form of a heatmap. (Heatmap generated through Python script)

Conclusion

Overall, natural flavanones are emerging as effective and safe psoriasis treatments. Flavanone-based therapies have the potential to change psoriasis management by combining encouraging docking results, outstanding safety profiles from ADMET studies, and reduced side effects—either as adjuncts or standalone therapy for patients seeking a holistic and well-tolerated strategy.

References

1. Yamazaki F. Psoriasis: Comorbidities. Vol. 48, Journal of Dermatology. John Wiley and Sons Inc; 2021. p. 732–40.
2. AlQassimi S, AlBrashdi S, Galadari H, Hashim MJ. Global burden of psoriasis – comparison of regional and global epidemiology, 1990 to 2017. Int J Dermatol. 2020 May 6;59(5):566–71.
3. Rahman M, Alam K, Ahmad MZ, Gupta G, Afzal M, Akhter S, et al. Classical to Current Approach for Treatment of Psoriasis: A Review. Endocr Metab Immune Disord Drug Targets. 2012 Jul 19;12(3):287–302.
4. Guo J, Zhang H, Lin W, Lu L, Su J, Chen X. Signaling pathways and targeted therapies for psoriasis. Vol. 8, Signal Transduction and Targeted Therapy. Springer Nature; 2023.
5. Pentu N, Rishitha P, Nikhil G, Rao TR. Therapeutic potential of flavonoids in the management of psoriasis. Asian J Pharm Pharmacol. 2024;10(1):35–45.
6. Billi AC, Gudjonsson JE, Voorhees JJ. Psoriasis: Past, Present, and Future. Vol. 139, Journal of Investigative Dermatology. Elsevier B.V.; 2019. p. e133–42.
7. Małgorzata Brodowska K. European Journal of Biological Research Natural flavonoids: classification, potential role, and application of flavonoid analogues. Eur J Biol Res [Internet]. 2017;7(2):108–23. Available from: http://dx.doi.org/10.5281/zenodo.545778

8. Lakshmi JN, Supriya P, Soumya PL, Vandana P, Narendra Babu A. Pharmacological Evaluation of Liquorice for Various Dermatological Disorders in Mice. International Journal of Pharmacy and Biological Sciences-IJPBS TM [Internet]. 2019;9(1):1253–9. Available from: www.ijpbs.comorwww.ijpbsonline.com

9. Pentu N, Bindu S, Rao R. Flavonoids: An Era Of Nutraceuticals Turning In To Medicinal Agents. 2024;17:2024. Available from: http://dx.doi.org/10.22159/ajpcr.2024v17i6.50514.

10. Khan MK, Zill-E-Huma, Dangles O. A comprehensive review on flavanones, the major citrus polyphenols. Journal of Food Composition and Analysis. 2014 Feb;33(1):85–104.

11. Alalaiwe A, Lin CF, Hsiao CY, Chen EL, Lin CY, Lien WC, et al. Development of flavanone and its derivatives as topical agents against psoriasis: The prediction of therapeutic efficiency through skin permeation evaluation and cell-based assay. Int J Pharm. 2020 May;581:119256.

12. Lakshmi JN, Narendra Babu A, Nadendla RR. Evaluation of anti-psoriatic activity of selected phytochemicals on uv-induced psoriasis in mouse tail model. Indian J Physiol Pharmacol. 2020 Apr 1;64(2):123–8.

13. De Souza Farias SA, Da Costa KS, Martins JBL. Analysis of Conformational, Structural, Magnetic, and Electronic Properties Related to Antioxidant Activity: Revisiting Flavan, Anthocyanidin, Flavanone, Flavonol, Isoflavone, Flavone, and Flavan-3-ol. ACS Omega. 2021 Apr 6;6(13):8908–18.

14. Rebello CJ, Beyl RA, Lertora JJL, Greenway FL, Ravussin E, Ribnicky DM, et al. Safety and pharmacokinetics of naringenin: A randomized, controlled, single-ascending-dose clinical trial. Diabetes Obes Metab. 2020 Jan 1;22(1):91–8.

15. Yin H, Li Y, Feng Y, Tian L, Li Y. The Extraction, Biosynthesis, Health-Promoting and Therapeutic Properties of Natural Flavanone Eriodictyol. Vol. 16, Nutrients . Multidisciplinary Digital Publishing Institute (MDPI); 2024.

16. Khodzhaieva RS, Gladkov ES, Kyrychenko A, Roshal AD. Progress and Achievements in Glycosylation of Flavonoids. Vol. 9, Frontiers in Chemistry. Frontiers Media S.A.; 2021.

17. Najmanová I, Vopršalová M, Saso L, Mladěnka P. The pharmacokinetics of flavanones. Vol. 60, Critical Reviews in Food Science and Nutrition. Bellwether Publishing, Ltd.; 2020. p. 3155–71.

18. Khan MK, Rakotomanomana N, Dufour C, Dangles O. Binding of citrus flavanones and their glucuronides and chalcones to human serum albumin. Food Funct. 2011;2(10):617.

19. Trott O, Olson AJ. AutoDock Vina: Improving the speed and accuracy of docking with a new scoring function, efficient optimization, and multithreading. J Comput Chem. 2010 Jan 30;31(2):455–61.

20. Rajesham V V., Pentu N, Kumar PK, Rao TR, Morsu A. In Silico Assessment Of Flavonoids From Matricaria Chamomilla For Anti-Psoriatic Potential Via Molecular Docking And Adme/T Profiling. Journal of Applied Pharmaceutical Research. 2025 Aug 31;13(4):162–76.

21. Valdés-Tresanco MS, Valdés-Tresanco ME, Valiente PA, Moreno E. AMDock: a versatile graphical tool for assisting molecular docking with Autodock Vina and Autodock4. Biol Direct. 2020 Sep 16;15(1).

22. Trott O, Olson AJ. AutoDock Vina: Improving the speed and accuracy of docking with a new scoring function, efficient optimization, and multithreading. J Comput Chem. 2010 Jan 30;31(2):455–61.

23. Hasan MM, Khan Z, Chowdhury MS, Khan MA, Moni MA, Rahman MH. In silico molecular docking and ADME/T analysis of Quercetin compound with its evaluation of broad-spectrum therapeutic potential against particular diseases. Inform Med Unlocked. 2022 Jan 1;29.

24. Kim OTP, Le MD, Trinh HX, Nong H V. In silico studies for the interaction of tumor necrosis factor-alpha (TNF-α) with different saponins from Vietnamese ginseng (Panax

Vol. 20 (Supplementary Issue 2A), June 2026, ISSN 0973-8916 (Print)., 2230-7303 (Online)
10.5530/ctbp.2026.2s.1

vietnamesis). Biophys Physicobiol. 2016;13:173–80.
25. V. V. Rajesham, Pentu N, Kumar PK, T. Rama Rao, Morsu A. In silico assessment of flavonoids from Matricaria chamomilla for anti-psoriatic potential via molecular docking and ADME/T profiling. Journal of Applied Pharmaceutical Research [Internet]. 2025 Aug 31;13(4):162–76. Available from: https://japtronline.com/index.php/joapr/article/view/1309
26. Lipinski CA. Lead- and drug-like compounds: the rule-of-five revolution. Drug Discov Today Technol. 2004 Dec;1(4):337–41.
27. Kowalska M, Fijałkowski Ł, Nowaczyk A. eISNN 2391-8306 The journal has had 7 points in Ministry of Science and Higher Education parametric evaluation. Journal of Education [Internet]. 2018;8(12):2391–8306. Available from: http://dx.doi.org/10.5281/zenodo.2066519
28. Sukhachev VS, Dmitriev A V., Ivanov SM, Savosina PI, Druzhilovskiy DS, Filimonov DA, et al. Assessment of the Efficiency of Selecting Promising Compounds During Virtual Screening Based on Various Estimations of Drug-Likeness. Pharm Chem J. 2024 Dec 21;58(9):1388–96.
29. Pentu N, Azhakesan A, Pasupuleti Kishore Kumar. Insilico molecular docking and ADME/T studies of flavonol compounds against selected proteins involved in inflammation mechanism. Journal of Applied Pharmaceutical Research [Internet]. 2025 Feb 28;13(1):95–111. Available from: https://japtronline.com/index.php/joapr/article/view/706
30. Lipinski CA. Drug-like properties and the causes of poor solubility and poor permeability.
31. Hasan MM, Khan Z, Chowdhury MS, Khan MA, Moni MA, Rahman MH. In silico molecular docking and ADME/T analysis of Quercetin compound with its evaluation of broad-spectrum therapeutic potential against particular diseases. Inform Med Unlocked. 2022;29:100894.
32. Pentu N, Azhakesan A, Pasupuleti Kishore Kumar. Insilico molecular docking and ADME/T studies of flavonol compounds against selected proteins involved in inflammation mechanism. Journal of Applied Pharmaceutical Research [Internet]. 2025 Feb 28;13(1):95–111. Available from: https://japtronline.com/index.php/joapr/article/view/706
33. Rarey M. Redocking the PDB. J Chem Inf Model. 2024 Jan 8;64(1):219–37.
34. Arango JPB, Rodriguez DYM, Cruz SL, Ocampo GT. In silico evaluation of pharmacokinetic properties and molecular docking for the identification of potential anticancer compounds. Comput Biol Chem. 2026 Feb 1;120.